ANALYSIS OF AUTOMOTIVE AXLE CARRIER ASSEMBLY AND COMPARISON WITH TEST RESULTS

by A.A. Herbert and A.O. Currie
Compumod Pty. Ltd.

and W. Wilson
Borg Warner Australia

ABSTRACT

This paper describes the analysis of an axle carrier manufactured by Borg Warner Australia for the Pontiac Firebird. The aims of the analysis were to model the separation of the crown and pinion gears under drive and coast load and to produce reasonably accurate stress information for the axle carrier shell. It was also intended to gain confidence in the modelling techniques so that they could be used in the design of future components.

Deflection test data was available for the actual carrier. The paper shows that good correlation (within the accuracy of the test) was achieved between the model and the test results.

This paper also discusses several other points of interest in the analysis. These include the use of solid modelling to define complex surface geometry, the use of inclined planes to model gear tooth interaction, modelling of bearing stiffness and support conditions and the use of thermal expansion to model an interference fit.

INTRODUCTION

The Borg Warner transmission and axle division in Australia is a major producer of automotive rear axle assemblies, automatic/manual transmissions and other manufactured automotive components. Once only supplying components to the Australian market, attractive exchange rates and an ability to produce components to exacting standards has led them to supplying automotive components in the world marketplace.

Borg Warner Australia manufactures the rear axle assembly of the Pontiac Firebird. It is the analysis of this component which is the subject of this paper.

The analysis had three basic aims;

i) To model the gear separation between the pinion and crown wheel under a variety of load conditions.

ii) To produce reasonably accurate stress data for the axle carrier casting.

iii) To gain confidence in modelling this type of structure so that the experience gained could be applied to the design of similar components.

Test data was available for the axle assembly in the form of a deflection test report and it was by comparing this with the results of the analysis that it was hoped to gain confidence in the techniques employed.

THE STRUCTURE

A photograph of the familiar type of live rear axle of the Pontiac Firebird is shown in Figure 1.

The axle consists of a malleable iron casting into which the axle tubes are pressed and plug welded. The axle is supported by coil springs on lugs offset behind the axle. The fore and aft motion is restrained by trailing arms and the torque reaction from the drive is resisted by a long reaction arm bolted to the nose of the carrier casting.

The differential housing is also a malleable iron casting, split at right angles to the axis of rotation. It carries the steel hypoid crown gear bolted to a radial flange. The differential housing and the pinion shaft are mounted on taper roller bearings.

Load is applied to the carrier differential assembly by three principal mechanisms. Firstly, in the manufacturing process, the axle tubes are pressed cold into the carrier casting. There is a fairly heavy interference fit between the axle tubes and the correponding bores in the casting. There is also an axial pre-load applied to the differential housing and pinion bearings.

The drive torque produces reaction forces between the pinion and crown gears which are reacted through the bearings and ultimately through the suspension and torque reaction arms.

Lastly, loads are applied to the ends of the axles by the drive traction forces and vehicle weight.

TEST DATA

An 'axle centre deflection test' had been performed by Borg Warner Australia on the axle in question. The test consisted of mounting the axle as shown in figure 2. Torque, body weight and tractive effort was applied to the axle and deflections measured at various locations on the gears and housing. The deflection transducers were mounted on a ring which was bolted to the carrier casting midway between the pinion bearings.

The results for this test for the drive and coast load conditions were available for comparison with the analysis results.

MODELLING STRATEGY

It was decided that, due to the complexity of the assembly, better results would be gained by analyzing the carrier in two parts, that is; the pinion shaft and differential housing as one model and the carrier shell as another.

For this approach it was necessary to assume that the parts could be uncoupled and that the bearings carried no bending moment.

The overall strategy adopted was;

a) To analyze the differential housing, ring gear and pinion shaft as a separate statically determinate structure, supported at the bearing centres for drive and coast torque loading on the pinion shaft. This model would include the axial flexibility of the bearings.

b) To analyze the axle carrier assembly supported at the suspension points with the following load cases applied;

The reaction forces from the bearing centres from step (a)

Traction and weight load cases for drive and coast.

Press fit loading from the assembly of the axle tubes.

This model would include the radial flexibility of the bearings.

c) To use the bearing centre deflections given by step (b) as a forced displacement load case for the differential model. (NB The deflections from the press fit load case were not included in the displacements used)

d) Finally to combine the deflection results from (c) with the deflection results from (a) to give total gear separation figures.

ANALYSIS

The analyses were performed using MSC/NASTRAN on a MicroVaxII. PDA/PATRAN II was used to create geometric models, create the finite element mesh, loading and boundary conditions and produce the MSC/NASTRAN bulk data decks.

Figures 3, 4 and 5 show plots of the finite element idealizations for the differential housing model and the axle carrier assembly model.

The differential housing model contained around 2000 nodes and consisted mostly of 8 noded brick elements with 3 degrees of freedom per node. The analysis took approximately 2.5 cpu hours for two load cases. The axle carrier model also contained around 2000 nodes but consisted of 4 noded quad elements with (approximately) six degrees of freedom per node. The analysis took approximately 5 cpu hours for three load cases. The scratch space required for each model fitted on one 70 MByte disk.

The analyses presented several points of interest. These are discussed below.

Load Transfer Between Pinion and Crown Wheel Gears (Figure 6)

The final aim of the analysis was to model the relative movement of the gear teeth at the mesh point between the crown and pinion. While it would have been adequate from the point of view of strength analysis to calculate the components of the contact forces between the gears and apply them to each gear separately, this would have had the effect of prizing the contacting faces of the gears apart. The resulting deflections would require subsequent modification to correctly reflect the gear movements.

Instead, the gear mesh was modelled as a sliding contact, correctly oriented at the contact point of the two gears. A local co-ordinate system was created at the contact point tangential to the gear surfaces. Two coincident nodes were created at this point connected by a spring element with stiffness only in the surface normal direction. The nodes were connected back to their respective parent structures with rigid links. It was necessary in this case to use separate models for the drive and coast load cases as the forward and reverse mesh angles are different. This method did also have the advantage, however, that the loading could be applied simply as a torque on the end of the pinion shaft.

Solid Modelling of Carrier Casting (Figures 7 & 8)

The carrier casting consisted of a very complex surface whose shape was dictated by the volume swept by the rotating gears. This surface was intersected by the tubes into which the axle tubes were pressed and was further complicated by tangential blends, fillet surfaces and sundry stiffening webs and flanges.

The authors were interested in using the recently released solid modelling facility in PATRAN II and this appeared to be an ideal application.

It had been decided to use QUAD4 elements for the casting so surface geometry was required for meshing. This was created by using a Boolean union operation to join the primitive solids shown in figure 7 and extracting the surface geometry (representing the mid-plane of the casting shell). The stiffeners were added as surfaces and the final geometric model shown in figure 8 was produced.

Bearing Seat Loading (Figure 9)

The analyst is often confronted with the problem of how to model an essentially non linear loading condition in a linear model. In this case it was the transfer of the radial and axial load from the bearings of the differential and pinion to the bearing seats. It was important that the deflection of the bearing centres was accurately modelled.

The reaction forces from the differental model were applied to nodes at the centres of the taper roller bearings. These nodes were connected to a coincident node by a spring element which had high stiffness in all directions except that parallel to the radial load vector. In this direction, the stiffness was equal to the radial stiffness of the bearing. The coincident node was in turn connected to the bearing seat in the radial direction by stiff ROD elements and in the axial direction by stiff spring elements.

The axial connection was made over 360 degrees of the bearing seat. The radial connection on the other hand was made to the 180 degrees of the bearing seat which faced the radial load vector.

The aim of this was to give a reaction to the radial load proportional to the angle between the bearing seat and the radial load vector and not to artificially restrain the bearing seat. It was thereby hoped to avoid the problems of a precalculated load distribution in which no account is taken of the different stiffnesses which may occur around the bearing seat.

Again, this technique necessitated having separate models for drive and coast load.

Interference Fit Loading (Figure 10)

During assembly of the axle, the axle tubes are pressed into bores in the casting. There is a heavy interference fit between the tube and the casting ie. 0.25mm over a diameter of 63mm. This imposes a high residual stress on the structure.

The inner end of the axle tubes was modelled with shell elements (the outer end degenerating to simple bars) and the interference fit condition was created by applying a thermal expansion to these elements. The axle tubes were connected to the cast bore around them with spring elements having a radial stiffness approximately equal to the radial stiffness of the tube wall.

RESULTS

Results were output from each analysis step as listings and as MSC/NASTRAN OUTPUT2 files for post processing in PATRAN. Deformed shapes and stress results were checked using PATRAN and the final combination of deflection results in step (d) of the modelling strategy was performed using the PATRAN results combination facility.

An extra complication arose in the analysis when it came to using the bearing deflection results as a forced displacement load case in the differential model. (Step (c) in the modelling strategy) The results contained large rigid body motions of the carrier due to the flexibility of the suspension and these, although they would not have affected the relative movements of the gears would have made comparison with the test results practically impossible.

A program was therefore written which transformed the displacements into a co-ordinate system defined by the displaced positions of selected nodes. The nodes chosen for the reference system were as close as possible to the reference data ring used in the test. These transformed displacements were used as the enforced displacement load set in the differential model.

A comparison of the relative gear movements from the analysis and from the test is shown in table 1. These deflections are for the combined bearing, traction and weight load on both the carrier and differential models. Two sets of figures are shown for the test results. The second set are movements linearly extrapolated from an earlier test at a lower torque. The inclusion of the second set gives some idea of the repeatability of the test and the linearity of the structure.

A diagramatic comparison of the analysis and test results is shown in figure 12.

Contour plots of Von Mises stress for the combined loading are shown for the outer and inner surface of the carrier casting in figures 13 and 14.

DISCUSSION

i) Deflection

It was possible to show from the analysis that the primary source of gear separation was bending in the pinion shaft. Other major sources of deflection were deformation of the differential bearing seats and, in the coast load case, axial flexibility of the differential bearings.

Inspection of the comparative gear movements in table 1 shows that reasonable correlation has been achieved between the analysis and the test. The most significant difference is in the last entry which represents the spreading of the differential bearing caps. It was realised that the model was probably inaccurate in the lateral movement of these components as the use of a shell analogy for the section was rather stretched at this point.

Examination of the deflection results led to the conclusion that the bearing stiffnesses used in the model were probably too high. The loadings in the bearings are well outside the limits of the manufacturers stiffness tables and the stiffness values were linearly extrapolated from the highest values. As the bearing stiffness had a significant contribution in the deflections of the gears it was considered important for further work that more accurate stiffness information be obtained.

The predicted test deflections in column 3 of table 1 were included to give some idea of the accuracy of the test data and the linearity of the structure. Clearly, although the predicted data is in good agreement with the final test data at some points, some non-linearity may exist or the accuracy of some readings may be poor.

The assumption was made in the modelling, that the gear contact point and contact angles would remain constant under load. In fact the gear contact changes significantly with tooth and gear deflection causing the contact point to move away from the theoretical contact point towards the heel or toe of the tooth. It is probable that this is a major source of non-linearity in the structure.

ii) Stress

Maximum stress in the carrier casting under service loads, that is excluding the residual stress caused during assembly, occurred in the seat of the rear pinion bearing. This was around 180 MPa. (See Figure 14).

The sheer bulk of the stress data makes it difficult to include much of the information in this paper. Stress results were not analyzed beyond pointing out the areas of highest stress under each loading condition and indicating those areas in which stress was very low and material might be saved.

The press fit load gave stresses in the axle tubes in excess of yield, showing that some yielding of these components must take place during assembly.

CONCLUSION

The analysis achieved the aims set out; to simulate the gear deflections and to provide stress results.

Indication was given of areas in which modelling could be improved, namely in the accuracy of bearing stiffnesses, in taking account of the change in contact point and angle in the gears under load and in the actual relation between interference and stress in the casting in the press fit condition.

The reasonable correlation between the analysis and test deflections gave confidence that the techniques used in this analysis could be used to predict and improve the performance of future designs.

ACKNOWLEDGEMENTS

The authors would like to thank the Borg Warner Company of Australia for the opportunity of presenting this work.

Table 1 - Comparison of Model and Test Relative Gear Movements

(Deflections in 0.001 ins.)

See Figure 11 for Interpretation

	F.E. Model	Test	Predicted
Fore and Aft			
Drive	11.9	12.1	12.7
Coast	-7.9	-13.1	-14.1
Vertical			
Drive	-19.4	-14.5	-13.9
Coast	19.2	19.1	20.1
Side			
Drive	-9.1	-11.2	-10.9
Coast	31.2	35.8	37.7
Axial			
Drive	4.3	8.4	6.7
Coast	4.8	-0.3	0.9

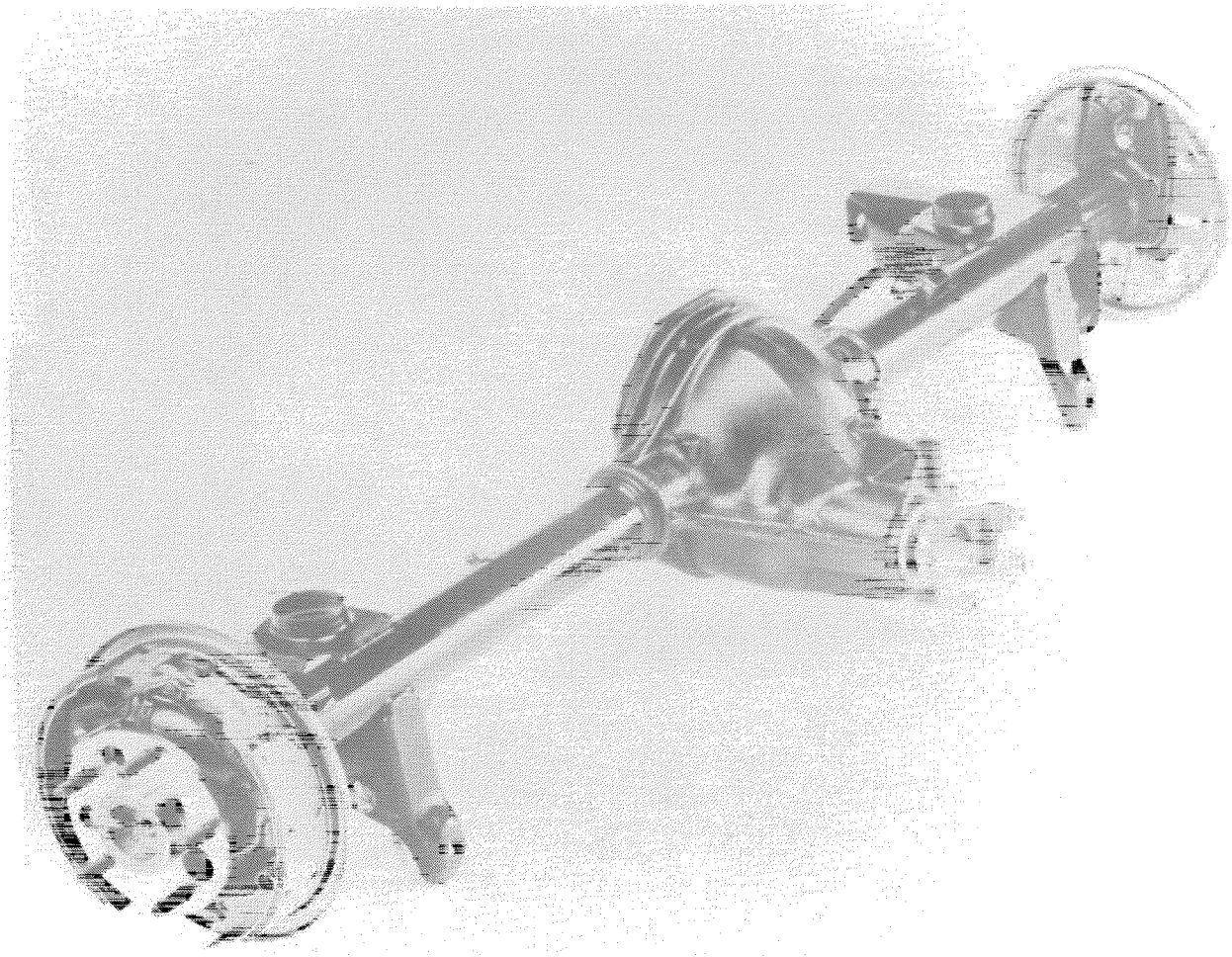

FIGURE 1 - BORG WARNER REAR AXLE FOR PONTIAC FIREBIRD

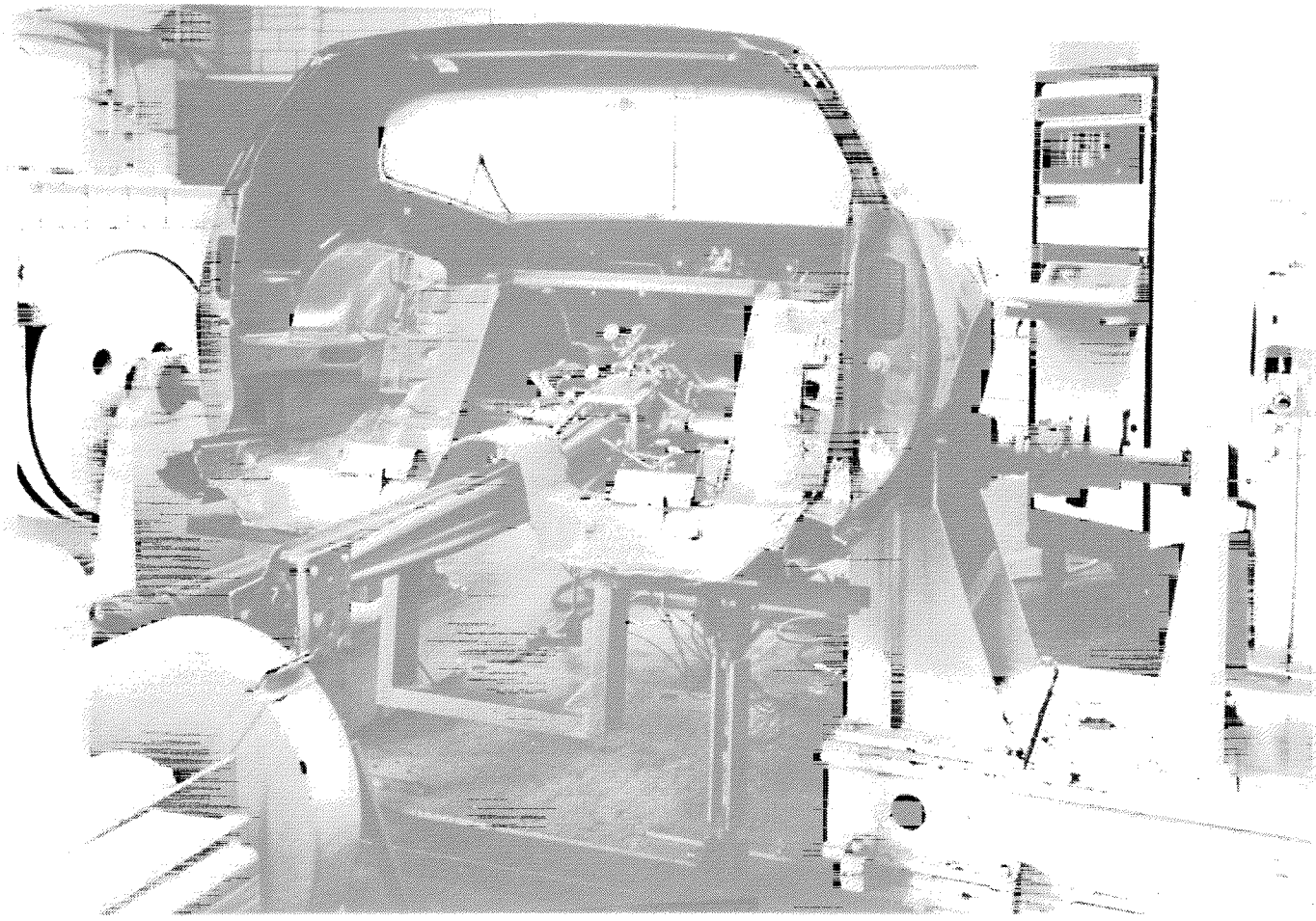

FIGURE 2 - AXLE CENTRE DEFLECTION TEST RIG

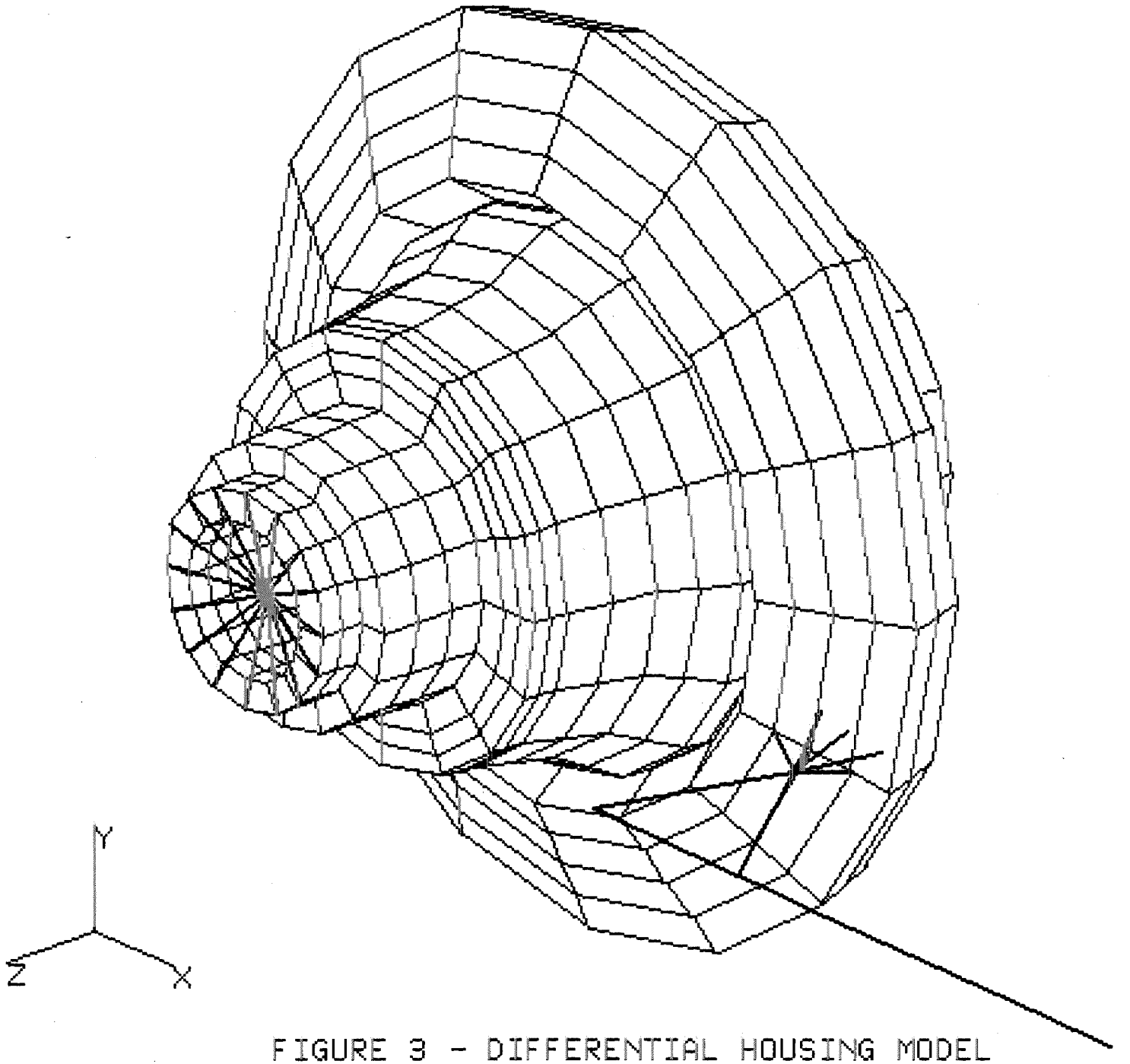

FIGURE 3 - DIFFERENTIAL HOUSING MODEL

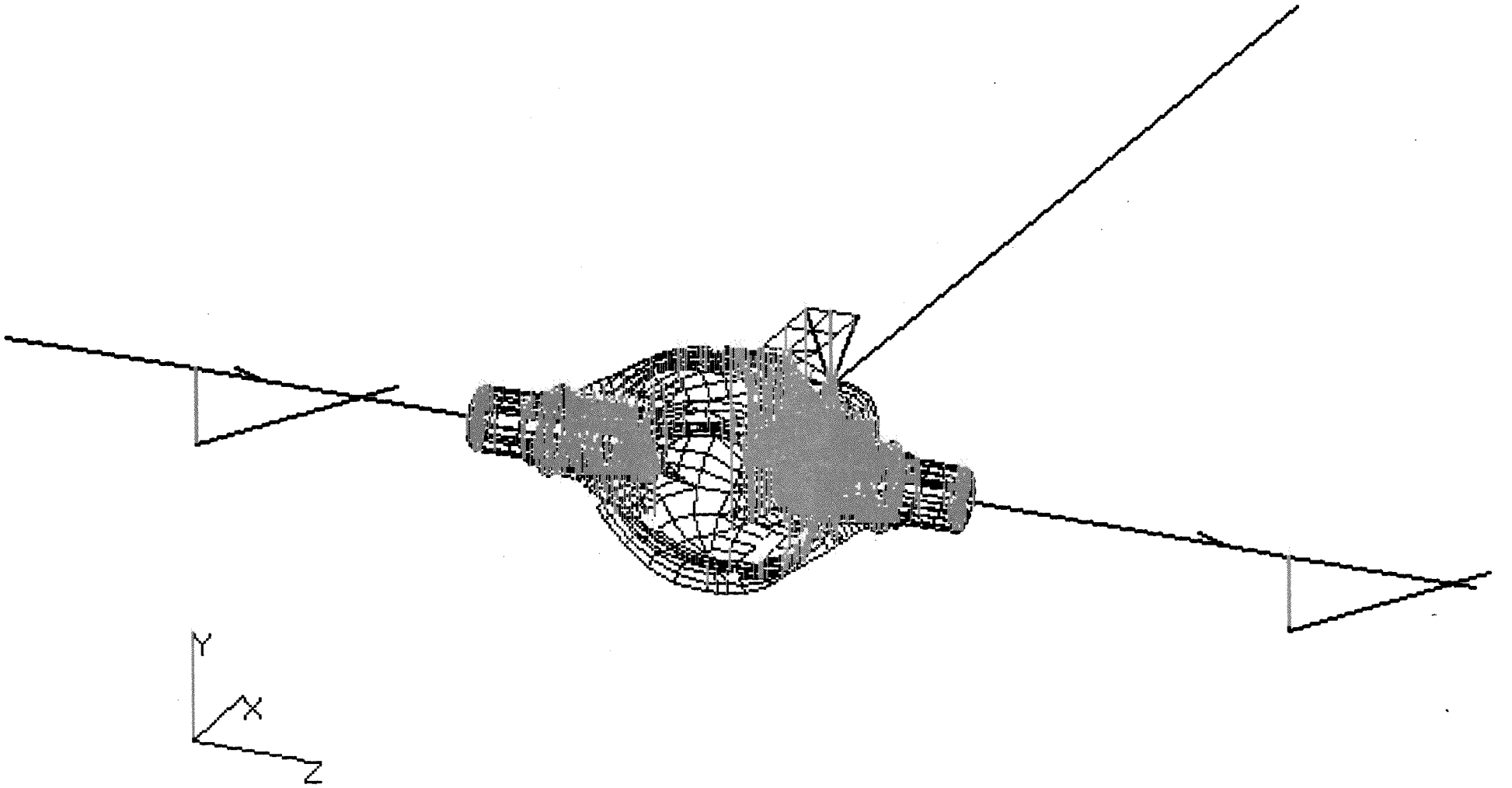

FIGURE 4 - AXLE CARRIER MODEL

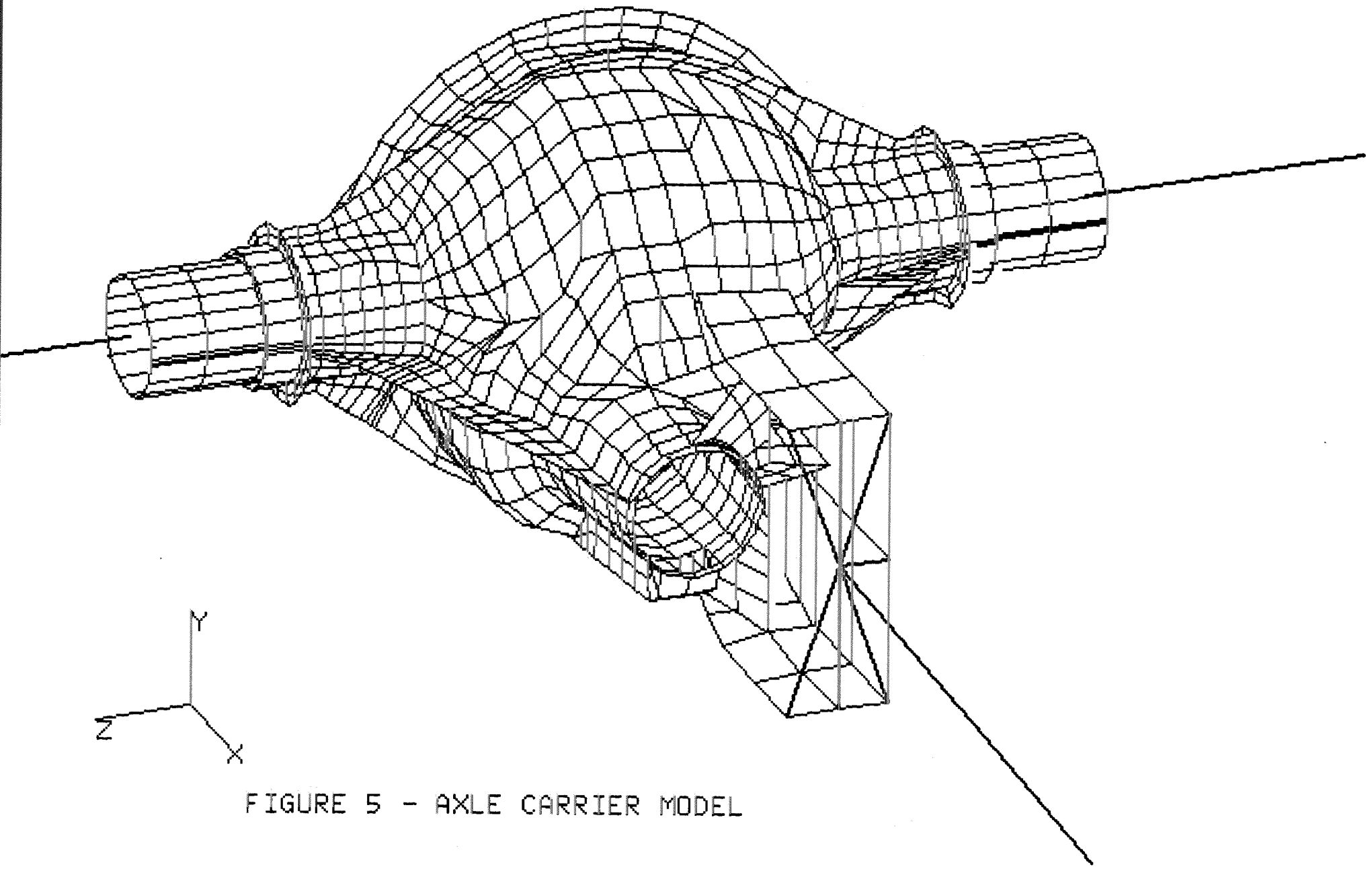

FIGURE 5 - AXLE CARRIER MODEL

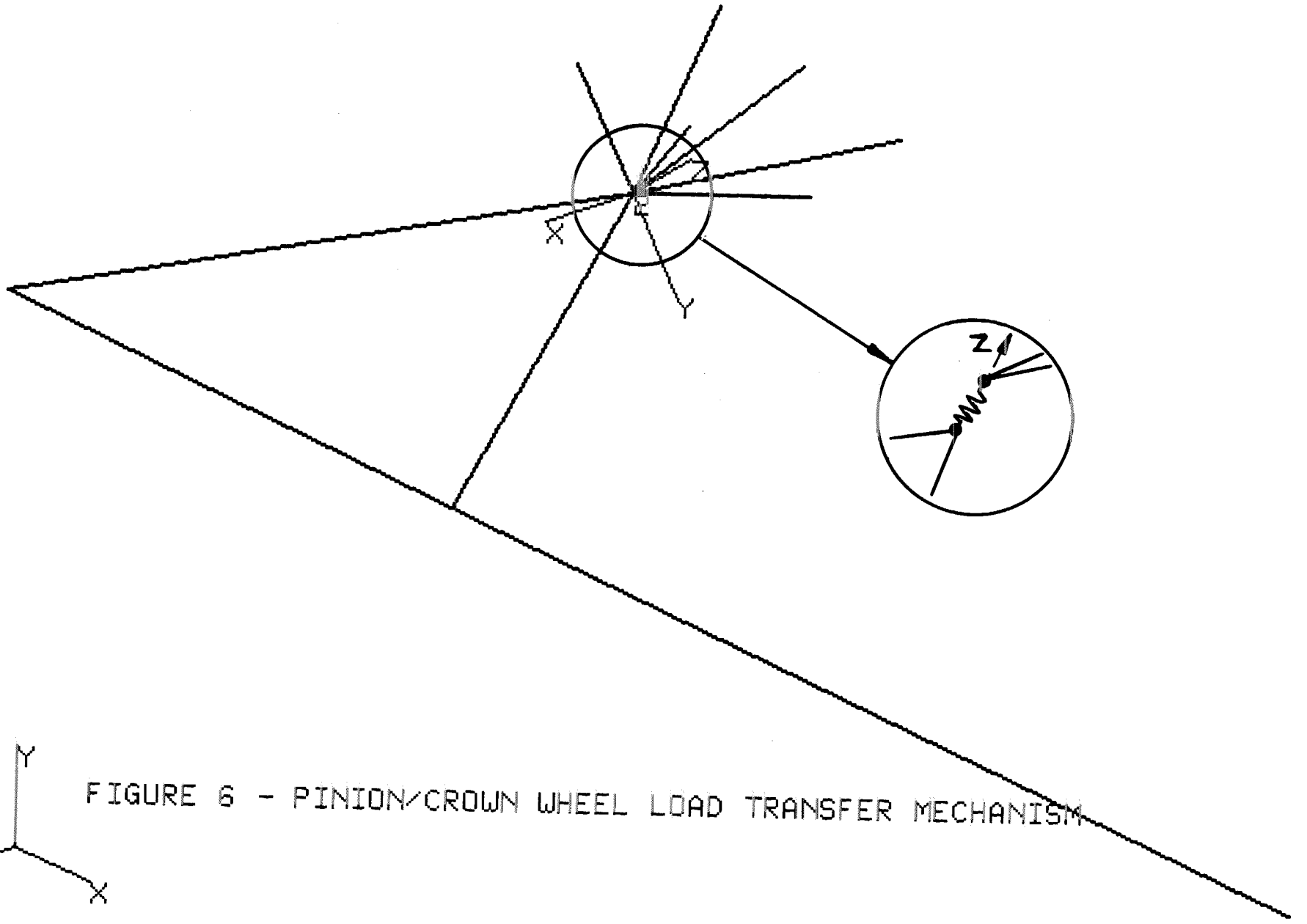

FIGURE 6 - PINION/CROWN WHEEL LOAD TRANSFER MECHANISM

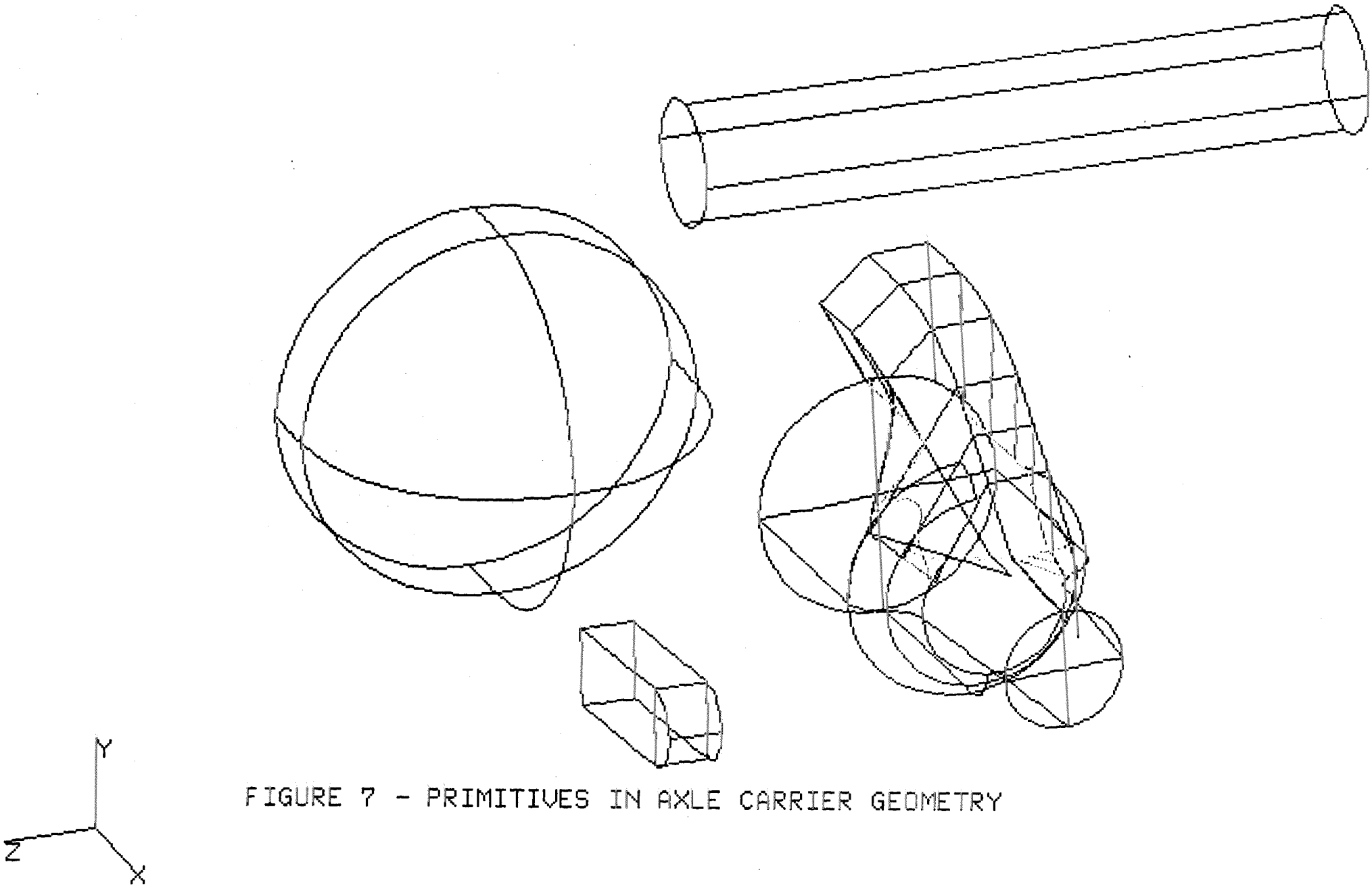

FIGURE 7 - PRIMITIVES IN AXLE CARRIER GEOMETRY

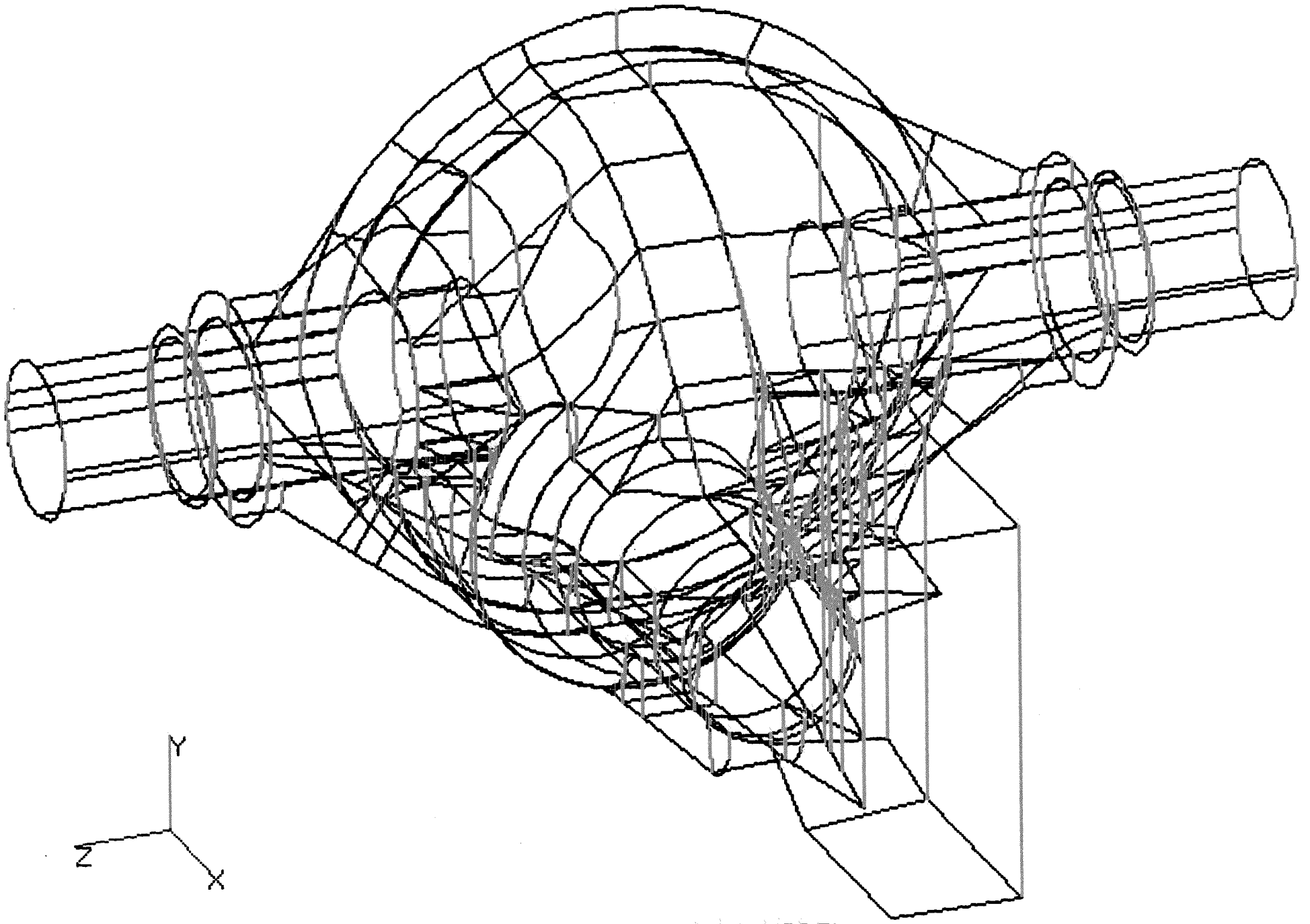

FIGURE 8 - COMPLETE GEOMETRIC MODEL

THRUST LOAD TRANSMISSION

RADIAL LOAD TRANSMISSION

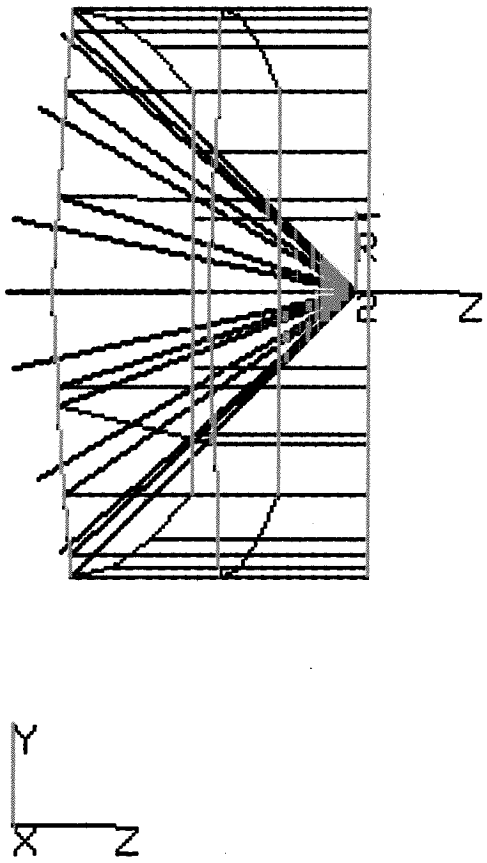

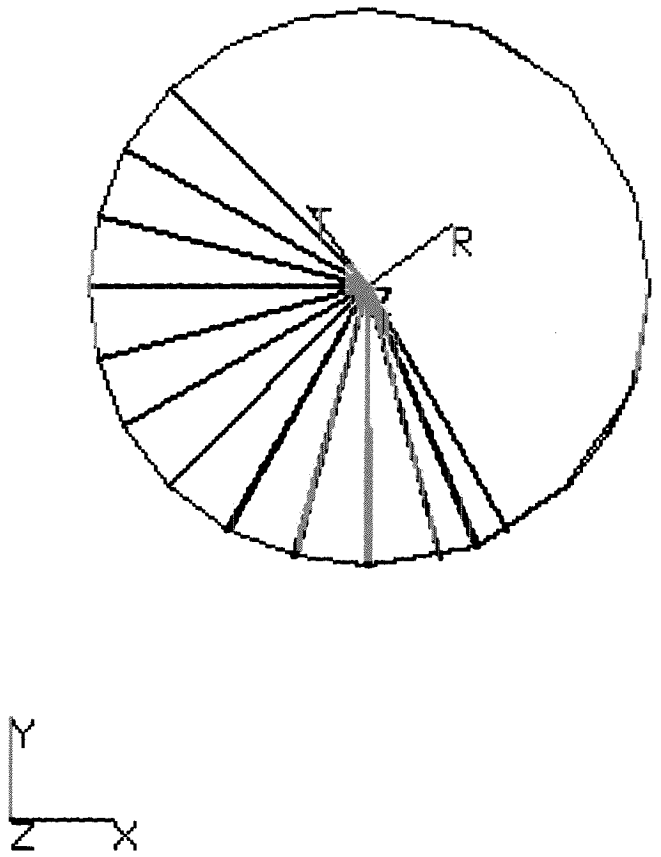

FIGURE 9 - BEARING SEAT LOAD DISTRIBUTION

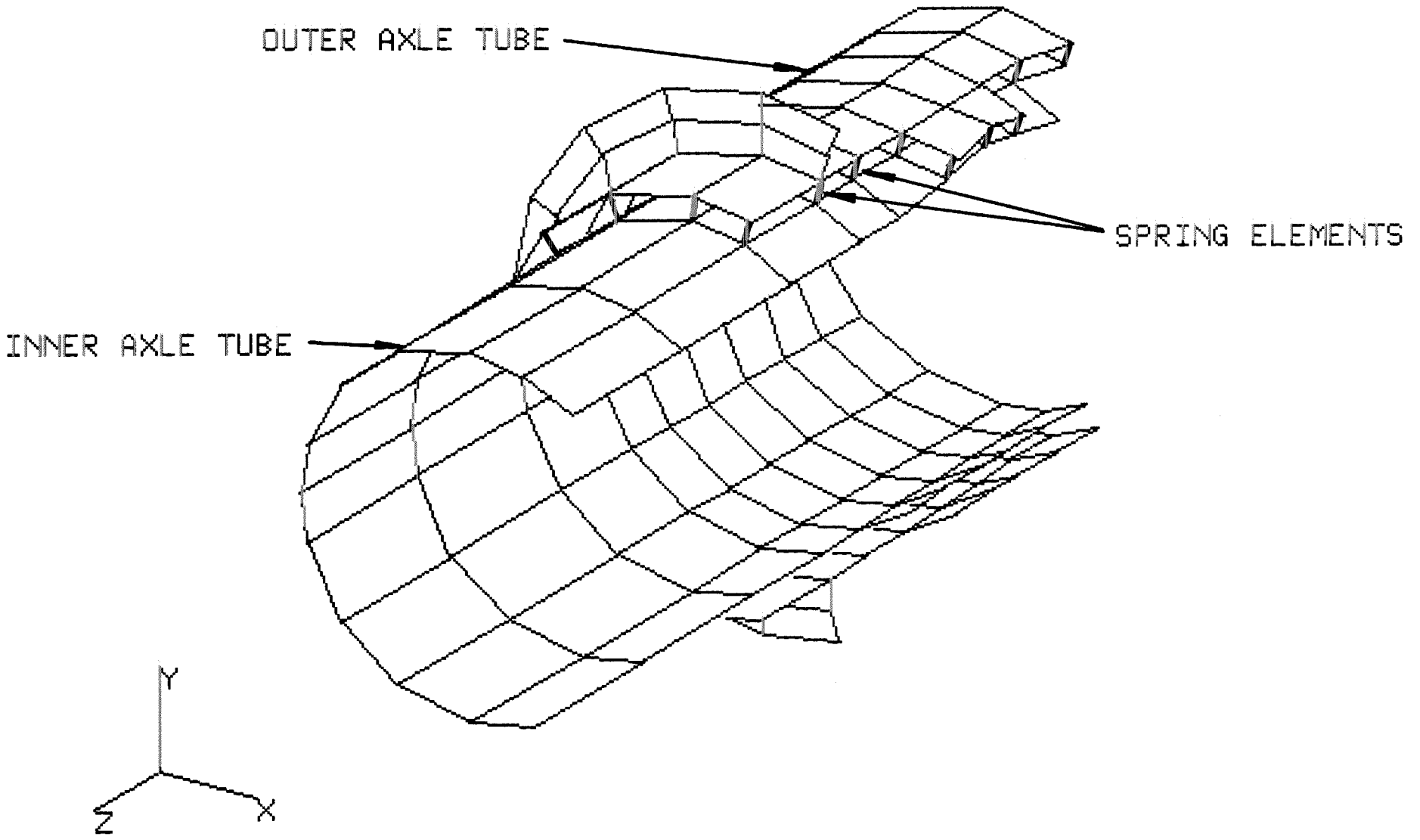

FIGURE 10 - DETAIL OF AXLE TUBE INTERFACE

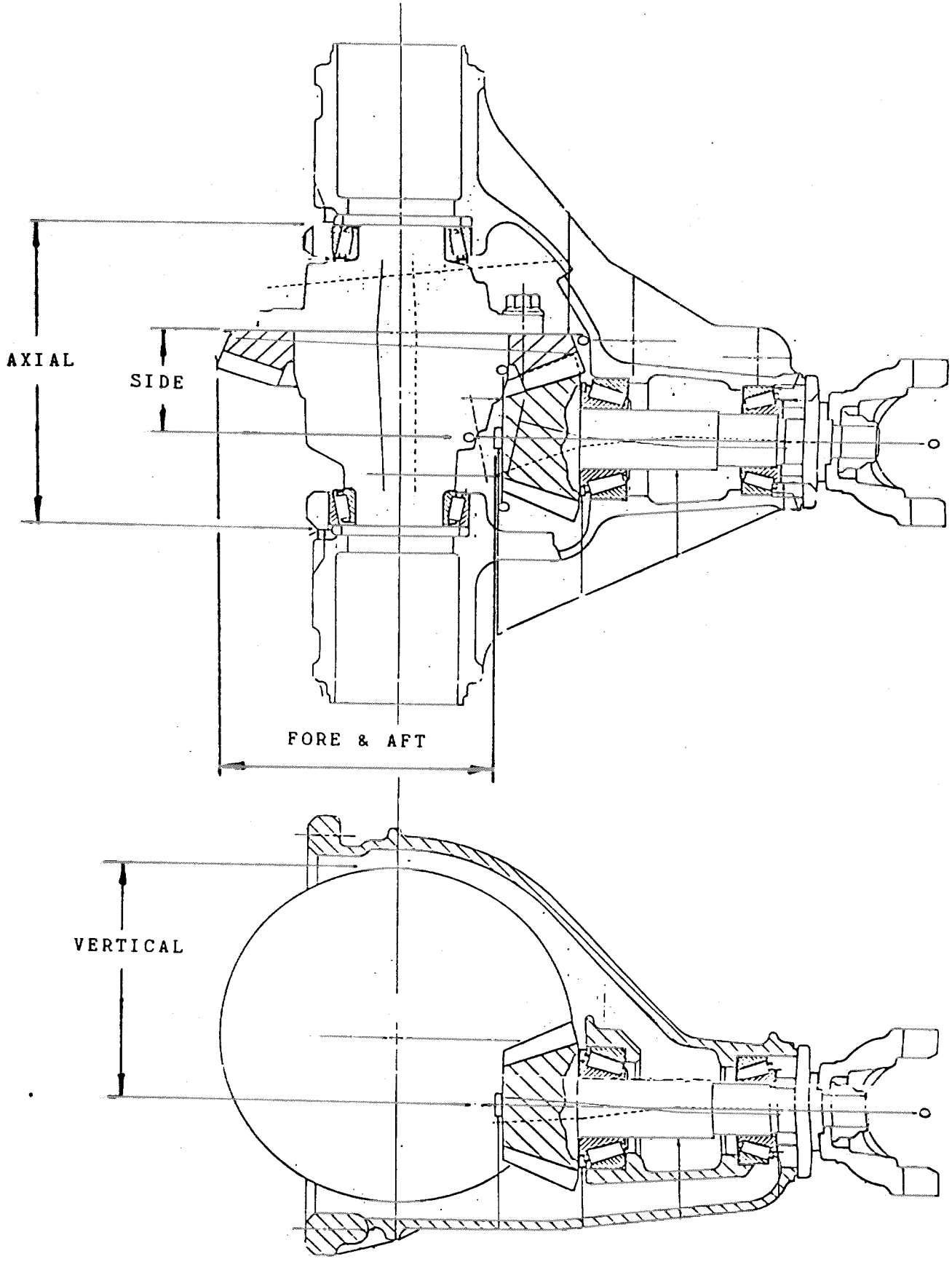

FIGURE 11 -- GEAR DEFLECTIONS

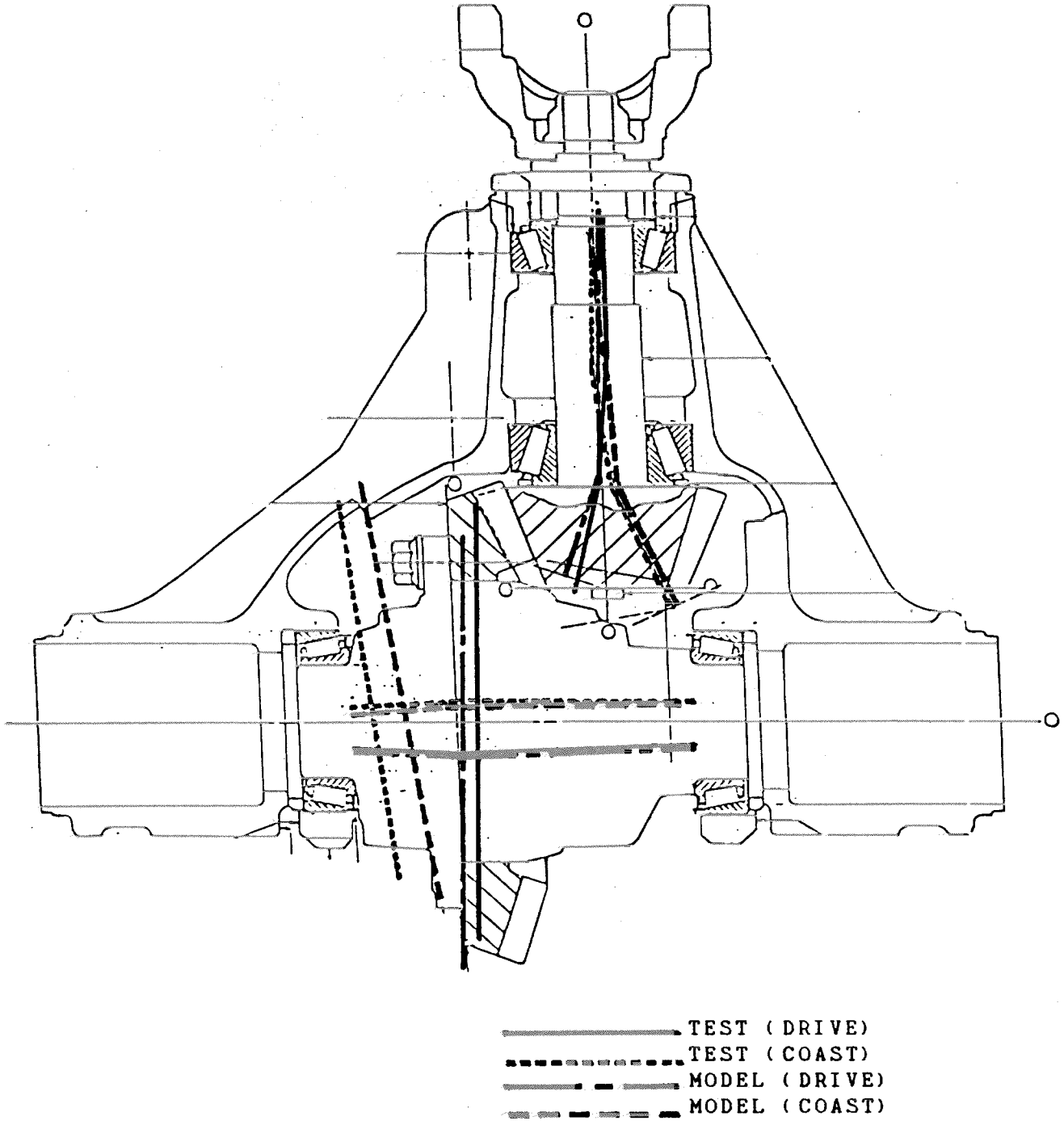

FIGURE 12 - COMPARISON OF ANALYSIS AND TEST DEFLECTIONS

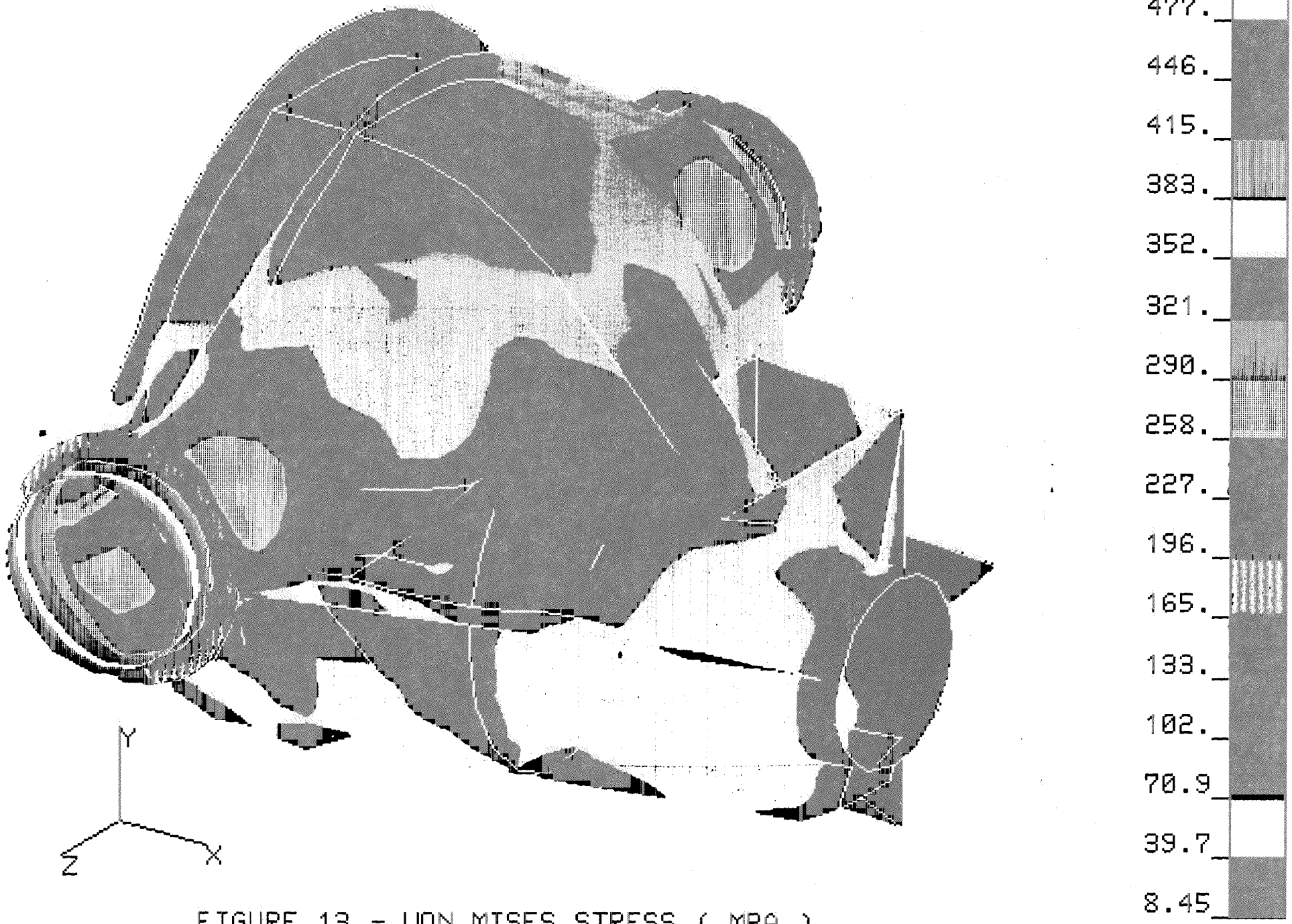

FIGURE 13 - VON MISES STRESS (MPA)
COMBINED LOAD CASE - OUTER SURFACE

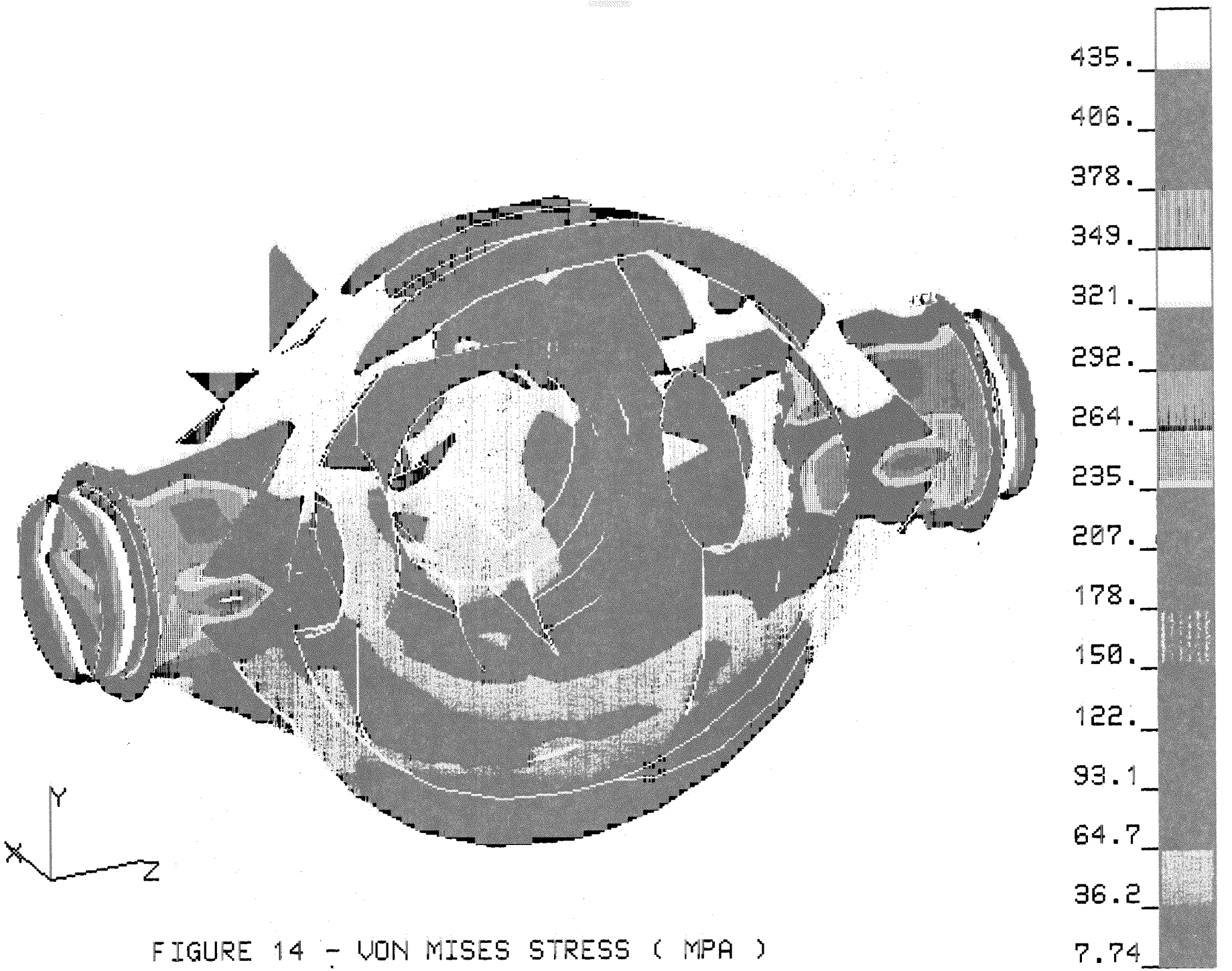

FIGURE 14 - VON MISES STRESS (MPA)
COMBINED LOAD CASE - INNER SURFACE